18th International Conference on Structural Mechanics in Reactor Technology (SMiRT 18)
Beijing, China, August 7-12, 2005
SMiRT18-G11-2

STRAIN-INDUCED DAMAGE TO PASSIVE FILMS ON AUSTENITIC STAINLESS STEELS

Paul Chard-Tuckey, Ken Trethewey, Mark Wenman, Sean Jarman
Nuclear Department, Defence College of Electromechanical Engineering, HMS Sultan, Gosport, Hampshire, PO12 3BY, United Kingdom.

Abstract

A full description is given of the new DASLER facility in the Nuclear Department. Four experimental series are described that explore the nature of the passive oxide film which protects stainless steels. It is demonstrated that failure of this film certainly occurs beyond the metal's yield point and repassivation competes with the generation of new substrate material in this dynamic process. Experiments have also shown that certain conditions will cause a breakdown of the film in the elastic region, through the mechanisms of crevice corrosion and pitting and it is the morphology of identified pits that are of particular interest.

Keywords: Passive films, Electrochemistry, Austenitic stainless steel, Damage, Rupture

1. Introduction and Background

Austenitic stainless steel (ASS) has been used for the past 40 years on primary circuit nuclear steam raising plant operated by the Royal Navy, with considerable success. The structural integrity of this material, which is subjected to high temperatures and pressures, needs to be assured. The failure mechanisms have been well researched and conditions have been established to optimise the performance of ASS in this application. However, a more complete understanding of the nature of the passive chromium oxide film is called for, partly driven by the requirement for continued plant life extension and also the advent of improved instrumentation and techniques that have become available in recent years.

This project explores the nature of the oxide film from a number of viewpoints, the data from which in combination, allow important conclusions to be drawn from these experiments and observations. Crucial to any experimental programme is a stable instrumented platform which is capable of generating precise traceable data in a reliable and repeatable fashion. Flexibility is also important, in that a wide range of experiments may be carried out using the same facility.

The Dynamic and Static Loading Electrochemistry Rig (DASLER) is an experimental facility in the Nuclear Department laboratories which combines a number of capabilities and for this series of investigations, allows ASS test specimens to be subjected to both dynamic and static loads in controlled environments, while collecting electrochemical signals which give a direct indication of the integrity of the oxide film at any particular instance. Hence, it is possible to draw some important conclusions about the breakdown of this film and the subsequent repassivation, as well as the kinetics involved in both cases.

A previous rig was constructed in the Department to carry out initial investigations and explore the feasibility of a number of experiments [1]. The main body of this strain rig consisted of two thick steel plates separated by four posts. A central hole through each plate accommodated the test specimen, which was secured in position by locking nuts on the outside face of each plate. Tension was applied to the specimen by means of tightening one of these nuts and the load produced reported in terms of nut rotation. The test specimen design was necessarily somewhat complex, in that the fabrication began with a 15mm diameter bar, threaded at either end, with the gauge length of rectangular section 80mm X 10mm X 3mm, formed by machining. A three electrode cell containing the electrolyte, was positioned on the upper surface of the specimen, sealed to the specimen by means of flexible tubing glued in position.

Following a very successful series of experiments, enhancements to this design were called for to allow for a simpler specimen design together with a more accurate idea of the load and extension experienced by the specimen, which could be recorded against the free corrosion potential.

The Nature of Oxide Films

Much research has been carried out into the nature of oxide films [2-5]. Stainless is an imprecise description but for steel to confer this characteristic, greater than 12% by weight of chromium is required. As the surface of the steel passivates and becomes less chemically active, a film of chromium oxide, Cr_2O_3 forms having a thickness no more than the order of tens of nanometres. Depending on surface exposure conditions, in particular, whether the film was allowed to form in air or an aqueous environment, one would expect a number of different oxides to be present. Iron and nickel oxides will exist to varying degrees within the chromium oxide matrix and the quantities present will relate to the rate of diffusion of these ions through the film in both directions and temperature is certainly an important factor here.

There are numerous proposed mechanisms for the form of corrosion known as environmentally-assisted cracking (EAC). Models that can predict the time to failure would be of great value, but are very difficult to create, given the diverse ways in which failures can occur for any given material/ environment combination. The mechanism deemed to apply in a given failure is derived from a combination of the crack morphology, i.e. transgranular or intergranular, and the mode of initiation, which could be from a strain-induced phenomenon or from a corrosion pit, for example. However, the initiation phase of EAC is the least predictable and many studies consequently assume an initiation time of zero and focus on the crack propagation phase. Hence, any new information relevant to the early behaviour of passive films on undamaged stainless steel surfaces is of considerable interest.

Many authors attribute the initiation of cracks in the strain-induced mechanism to the formation of slip steps and the rupture of passive films due to the emergent dislocations. By definition, these events take place after the onset of plastic deformation. However, oxides can fracture at strains where the deformation of the metal is still elastic when the fracture stress of the oxide is lower than that of the substrate metal. It is accepted that a damaged film will undergo a self-repair mechanism by reaction with water molecules, if not by direct oxidation by dissolved oxygen. Thus, under constant load, it is assumed that the film undergoes self-healing, but the data in this paper shows that under certain loading/environmental conditions - even below the yield stress -rupture of the passive film occurs which allows the creation of identifiable crack initiation sites such as pits.

Principles of Electrochemistry

The electrochemical series gives an indication of the propensity of various metals to corrosion. More precisely, the electrochemical series is built up by arranging various redox equilibria in order of their standard electrode potentials (redox potentials). Metals having large negative values readily lose electrons forming metal ions in a process of oxidation. Conversely, those metals having large positive values have ions which readily accept electrons to form the solid metal in a process of reduction. Hence, it is the passage of these electrons which yields the current density, the direct measure of corrosion. For the chromium reaction:

$4Cr \rightarrow 4Cr^{3+} + 12e^-$ and hence,

$4Cr^{3+} + 12e^- + 3O_2 \rightarrow 2Cr_2O_3$.

Here we are concerned with metals in an aqueous environment. The electrochemical potential (E_{Corr}, the corrosion potential) which a metal develops against some reference potential, will result in either a stable inert state (immune), dissolution and free corrosion of the metal (active), or the generation of a stable protective oxide film (passivation). However, E_{Corr} will vary with the composition of the environment, including chemical gradients, by subtle changes in the alloying components of the base metal and through the presence of cracks and crevices. In the case of passivating metals such as ASS, E_{Corr} will also vary considerably with the amount of surface preparation and the elapsed time of exposure to the atmosphere since that preparation process.

Under dynamic loading conditions, it is expected that the oxide film will be disturbed and the extent of this physical change will be manifested by a change in the free corrosion potential, E_{Corr}. There will clearly be some competition between the stresses causing a failure of the film, giving a fall in E_{Corr} and the mechanism of repassivation, which heals the surface, giving a rise in E_{Corr}. Under a static load, crevice corrosion and pitting, which both disturb the oxide film, will cause changes in E_{Corr}. In the case of a small pit, repassivation is expected to occur but insofar as a large pit or crevice is concerned, this may develop into wider activity across the surface, with a consequent fall in E_{Corr} as more gross corrosion takes place and larger areas of fresh metal are revealed.

2. Description of DASLER

The Load Frame
The load frame is based around a 20 kN (2 tonne force) Monsanto horizontally configured arrangement, which is most suitable for the testing of small section tensile test specimens within the laboratory. This calibrated facility is capable of imposing static and dynamic loads based on a constant strain rate from around 30 μm/sec to 400 μm/sec. During a test, digital displays give load and extension data and these are usually output to an X-Y plotter to display the test output data in the familiar stress-strain form. The load is applied via a lead-screw and a micrometer in contact with the head gave a secondary output of the strain on the specimen. To begin a test, a specimen was loaded together with modified tooling and attached by the clevis pins to the attachment at the head of the lead-screw and the static attachment connected to the 20 kN load cell. The slack in the assembly is taken up until the load cell output just begins to give a non-zero output. Experiments could then proceed, be they at constant strain rate or load and hold.

Load and Extension Data
As previously mentioned, the Monsanto load frame gives a front panel display of load in kN and extension in mm. An analogue output of these data is available and for this series of experiments it was necessary to log these data. For this purpose, a LabJack U12 data acquisition interface having an analogue to digital converter (ADC) was employed, with a resolution of 12 bits (4096) across the load and extension ranges. Input to the data logging computer was by a standard USB port. The as-supplied code allowed gain and offset parameters to be adjusted to yield actual load and extension values.

The Test Specimens
As with previous experiments reported at [1], austenitic stainless steel of type A304 S11 was employed to fabricate the test specimens. The composition of the steel was as follows: C 0.03%, Si 1.00%, Mn 2.00%, P 0.045%, S 0.030%, Cr 17-19%, Ni 9-12%, with the balance being Fe. The as-delivered steel was provided in 1m X 2m plate form of thickness 3 mm and having a fine brushed surface finish. A new design of test specimen with a gauge length of 120 mm, width 8 mm and thickness 3 mm was specified with tolerances of 100 μm. Individual specimens were laser cut from the plate by computer control and hence, the specimen-to-specimen variability was minimal. Although producing unconventional rectangular-section tensile specimens, this process was capable of producing large numbers of specimens, having consistent properties and geometries, whilst being fabricated at low cost.

Specimen Surface Preparation
The as-supplied austenitic stainless steel plate had a fine brushed surface finish. As this series of experiments was specifically targeted at an investigation of the surface film, it was important to observe and note the surface condition. Additionally, some idea had to be recorded of the time since surface preparation, as the specimens would continue to passivate in air until the actual experiment was performed. The highest level of polishing often involved a combination of abrasive wheels and hand finishing using 600 grade or higher wet and dry paper. It was only necessary to polish the specimens on a single side and in the region where the electrolytic cell was to be positioned.
To check the electrochemical data and the experimental procedures, one specimen was placed in an Edwards coating facility and the surrounding volume evacuated to a near vacuum. A molybdenum crucible was loaded with pieces of 0.5 mm thick gold plate and electrically heated to melt and vapourise the gold. Gold vapour is released and disperses essentially in a straight line from the point-source crucible, coating the unmasked section of the specimen. For a satisfactory film of gold, the polished specimen needs to be thoroughly cleaned with acetone and the heater current controlled to give a slow deposition. Improvements can be made by re-cleaning the specimen and applying a further coat.

Tooling Design
To accommodate the design of the new tensile test specimens, it was necessary to design appropriate tooling for the load frame. At either end of the specimen, two rectangular rebated steel plates are positioned and located above and below the specimen to be tested. The specimen is hence sandwiched in between and held by pairs of screws and locknuts. These screws pass through 10 mm diameter steel posts and it is these posts which transmit the load to the test specimen. In its assembled form, the tooling has circular holes in each end which connect to the load frame in the conventional manner by means of a single clevis pin at either end.

The Electrolyte Cell
The design of the cell to contain and seal the appropriate electrolyte above the test specimen surface, while allowing access for electrodes, required some ingenuity. The final design was machined from Perspex and 45 mm diameter with a height of 20 mm, having an interior of conical form with a 3 mm diameter hole at the base. A single

o-ring of internal diameter 5 mm sealed the fluid below this hole and was positioned in a machined slot under the cell body and sat proud of the Perspex surface. A removable clamp held the cell in position, while allowing the o-ring to be tightened onto the upper specimen surface by a plastic bolt carefully hand-tightened onto the underside of the specimen, thus clamping the whole arrangement in place.

The cell could then be filled with a pipette and a final pumping action ensured any bubbles were cleared from the surface of the metal. Retort clamps were positioned to allow the reference and counter (platinum wire) electrodes access to the electrolyte and the working electrode was attached firmly to the specimen. This series of experiments used sodium sulphate and potassium chloride as electrolytes, depending on the test being conducted

The Reference Electrodes
Two kinds of Standard Reference Electrodes were employed for this series of experiments. Firstly, a Silver-Silver Chloride (SSC) electrode having a AgCl/3M KCl interface and secondly, a Calomel electrode (SCE) with a Hg/3.5M KCl interface. With respect to hydrogen, the SSC has a reference voltage of +0.222 volts while the SCE has a reference voltage of +0.242 volts. It is well known that chloride ions have a detrimental effect on ASS and to ensure there was no contamination of the electrolyte by chloride ions from the reference electrode, for some experiments the KCl was replaced with K_2SO_4 . Of course, this non-standard electrode required calibration against a standard cell before every use and was found to be in the range +0.043 to +0.106 volts.

Electrochemistry Instrumentation
The instrumentation used to carry out the electrochemical aspect of the experiments was based around an Autolab potentiostat and galvanostat The dedicated code driving this instrument has a wide range of electrochemical functions and procedures. The selected procedure follows a reasonably standard technique, employing the use of a standard reference electrode, a platinum wire counter electrode, both in contact with the electrolyte cell fluid and a working electrode connected to the actual specimen surface. The free corrosion potential E_{Corr} is the voltage between the reference and working electrodes.
Damage to the oxide film reveals the fresh metallic substrate below and causes a depression in the free corrosion potential and an increase in the consequent current. The start and finish values of these parameters, give an indication of the degree of initial passivation or preconditioned state of the surface together with an indication of the extent of damage to the film caused by the actual loading regime and environment being explored.

The Cell Electrolyte
Before each test the electrolytic cell was carefully filled with electrolyte. In earlier experiments, 0.1M sodium sulphate was used. In later experiments potassium chloride was used in the range 1 ppm to 35,500 ppm (1M), the chloride ions providing a more challenging environment for the austenitic stainless steel.

Microscopic Observations
Specimens have been optically observed pre and post-test. A Leitz cohler-illuminated binocular materials microscope was used for many of these observations and images recorded by means of a Leica DC150 photomicrography system comprising a Canon five megapixel digital camera mounted above the microscope, using specialised coupling optics which align the focal plane with the CCD. Images of a calibration test piece recorded at various magnifications allowed features and indications on subsequent micrographs to be scaled.
A Jeol Scanning Electron Microscope (SEM) with an accelerating voltage of 30 kV was used to make careful detailed examination of features of interest discovered during Leitz microscope observations. An additional feature of the SEM is an EDX facility which translates the x-rays generated by the motion of specimen shell electrons following disruption by the high energy SEM electrons, into an elemental analysis of the sample. Surface maps showing the distribution of the various elements may then be displayed, yielding clues to the nature of features found on specimens.

3. Experimental

Initial Experiments
To check for the satisfactory operation of the load frame and the new design of tooling, and to especially characterise the new tensile specimen design, a constant strain rate test was carried out to ultimate failure of the specimen. A strain rate of 50 μm/sec was selected and a stress-strain curve was generated from the data (Fig 1). Yielding occurred at a load of 7 kN giving a yield stress of 292 MPa. The Ultimate Tensile Stress (UTS) of 734 MPa occurred at a load of 17.6 kN (well within the 20 kN range of the load frame). Finally, the strain at failure was some 67%.

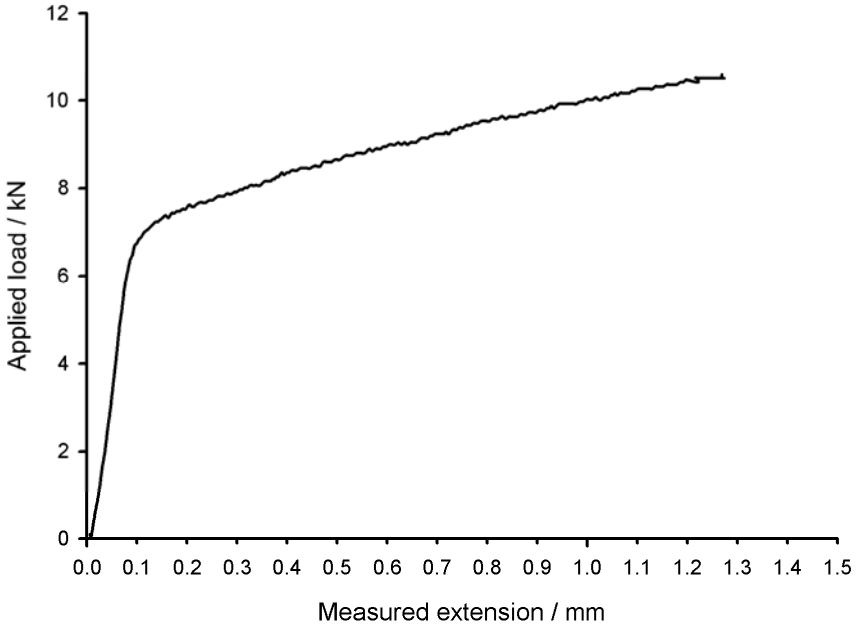

Figure 1

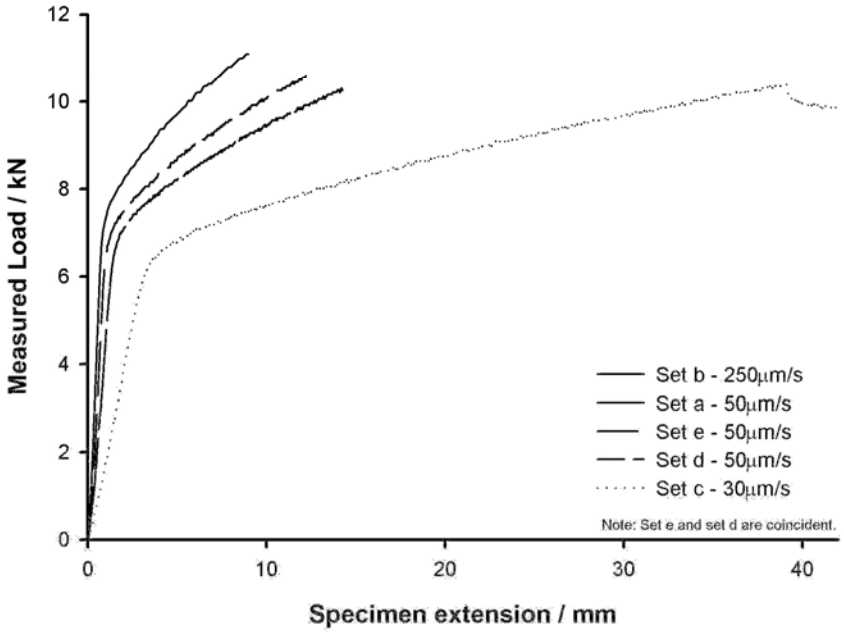

Figure 2

Series One Tests

This series of experiments was based on constant strain rate tests from zero load to about 10 kN, well beyond the elastic limit into yield. The specimens were mostly polished, with different subsequent passivation times. Records were logged of the open circuit potential, E_{Corr}, and the load and strain data. On closer inspection, the strain data from the ADC appeared somewhat noisy and thought to be unreliable. As time is one of the logged parameters, for a constant strain rate test, the actual strain at any particular instant could be determined. The SCE standard reference electrode was loaded with potassium sulphate and calibrated against a standard cell, giving an offset voltage which needed to be applied to the subsequent data. The electrolytic cell was loaded with the same electrolyte and hence the tested specimens were being exposed to a fairly benign environment.

The strain rates used for these experiments were in the range 30 μm/sec to 399 μm/sec. One observation is with regard to the stress-strain curves (Fig 2). As the strain rate is increased, there is a consequential increase in the yield stress and other parameters. Testing standards (BS EN 10002-1:2001) give advice on appropriate strain rates when carrying out tensile tests to generate valid materials property data. Based on a 120 mm gauge length, the strain rate range used in this series of tests translates into a range from 25 X 10^{-6} %/sec to 330 X 10^{-6} %/sec. The lower end of this range is in keeping with the test standards but as these experiments involved higher strain rates, it was important to generate these curves, and consequently know the yield stress for a particular strain rate. For this series of tests, the data logging commenced on the potentiostat and following a settling time for E_{Corr}, the load frame sequence was initiated.

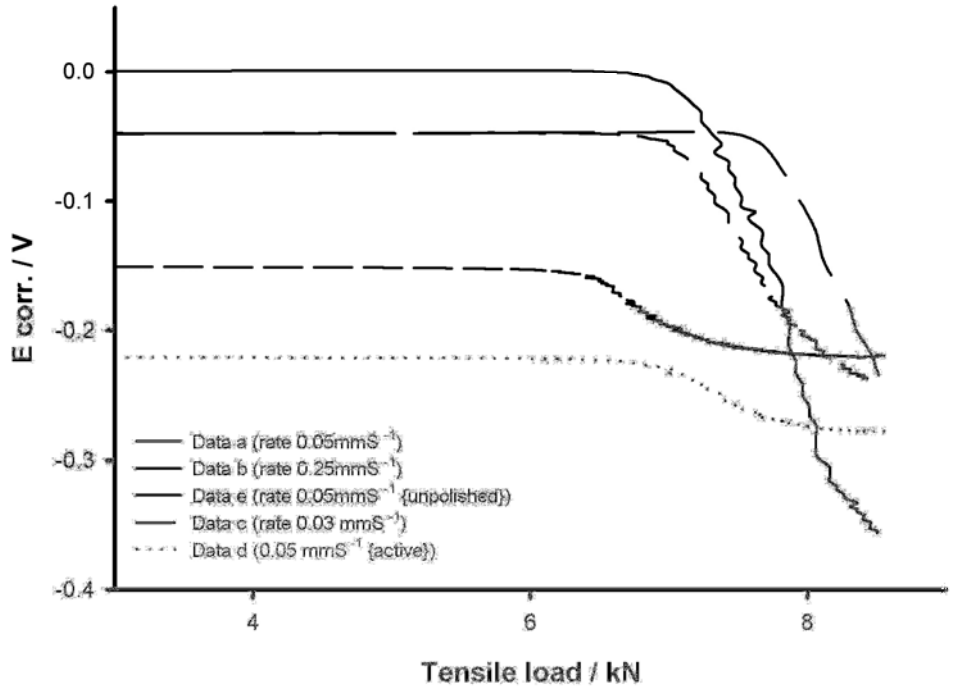

Figure 3

Of particular interest was how E_{Corr} changed as the load increased (Fig 3). In this context, E_{Corr} is being used as an indicator of the metal surface activity resulting from disruption of the oxide film. The figure indicates a number of interesting features. The initial value of E_{Corr} depends on the degree of surface passivation. Hence, a freshly prepared specimen exhibits greater surface activity indicated by a high negative value of voltage. A similarly prepared specimen which had been allowed to passivate in air for some weeks, exhibits a less negative potential and is sometimes even positive (Fig 4).

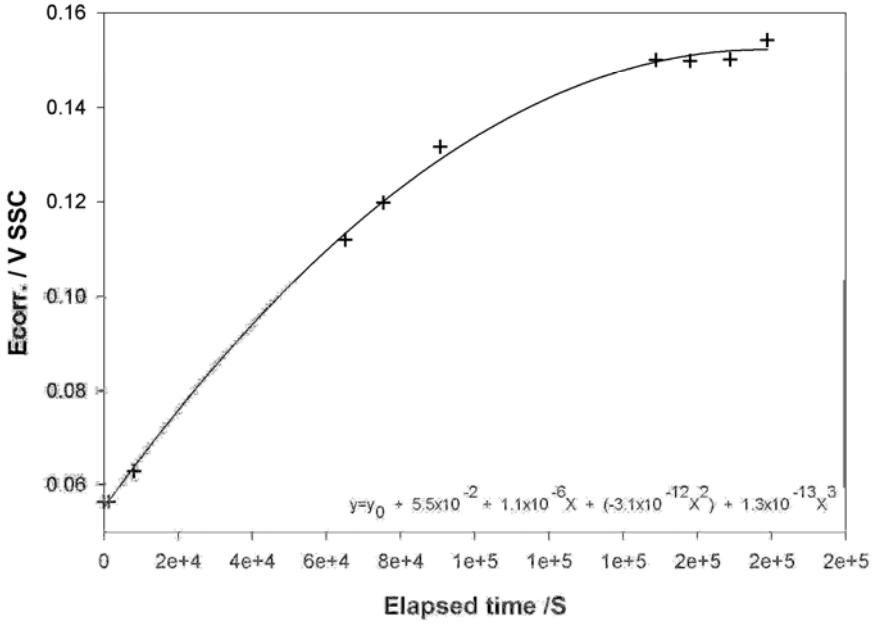

Figure 4

For all tests in this series, the free corrosion potential goes more negative as the load and hence stress is increased beyond yield. A measure of the damage to the surface film is related to ΔE_{Corr}, which is the total depression over the test of E_{Corr}. As can be seen, for those specimens with a substantial passive layer, the disruption to the film is large with ΔE_{Corr} the order of hundreds of millivolts. The more recently prepared surfaces, although starting with a depressed E_{Corr}, suffer a smaller damage as the film is thinner in the first instance. During the test, the stress at the point which E_{Corr} begins to fall is beyond the yield stress of the substrate material. This suggests that no damage occurs to the oxide film at any reasonable strain rate, in the elastic region. Of course, the stress at the point at which E_{Corr} begins to fall does rise as the strain rate increases but this is an artefact of the effect on the stress-strain curve mentioned earlier. Hence, a more passive, thicker film will suffer more damage on rupture but it is necessary to strain the material beyond the yield stress to do so.

Series Two Tests

This series of tests was carried out to investigate further, interesting anomalies on the E_{Corr} signal which had been noted earlier (Fig 5). Also, to make a further check on whether film damage was truly a post-yield phenomenon. A very high strain rate test (399 μm/sec) involving load/unload cycles, revealed no substantial change in E_{Corr} for loads below the yield point. Noted during the hold periods however, were small (order of a millivolt) sudden changes in the E_{Corr} signal. This might be confused with noise on the signal but careful examination shows that these sudden events are mostly in a negative direction, suggesting a temporary activation of the surface which decays back towards the general signal trend. This is thought to be caused either by pits forming and reactivating on the surface or crevice corrosion occurring in the region where the o-ring seal makes contact with the metal surface.

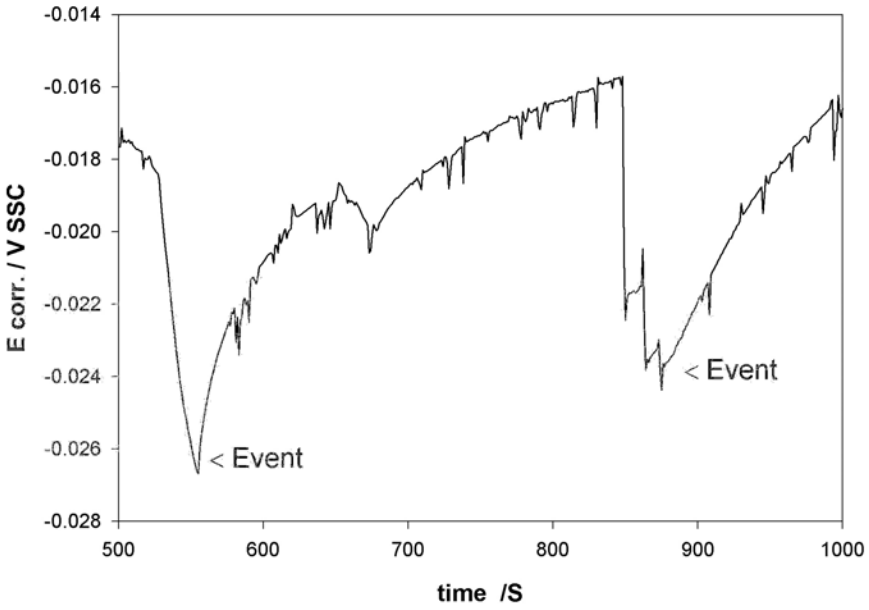

Figure 5

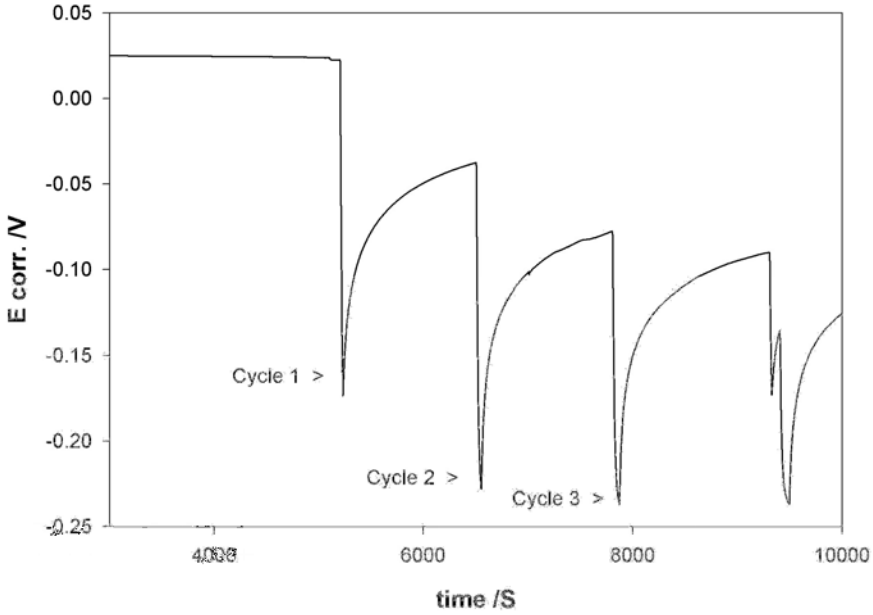

Figure 6

An experiment was carried out to analyse the repassivation process following rupture of the passive film. The specimen was subjected to a staircase-type load and hold sequence, which continued well into yield. Fig 6 shows the immediate effect on E_{Corr} of incrementing the load with a sudden depression in this voltage as the passive film ruptures and reveals the fresh substrate material below. This is followed by a recovery period, indicating surface repassivation. The three repassivation cycles shown in the figure were subsequently plotted together on a logarithmic time base (Fig 7).

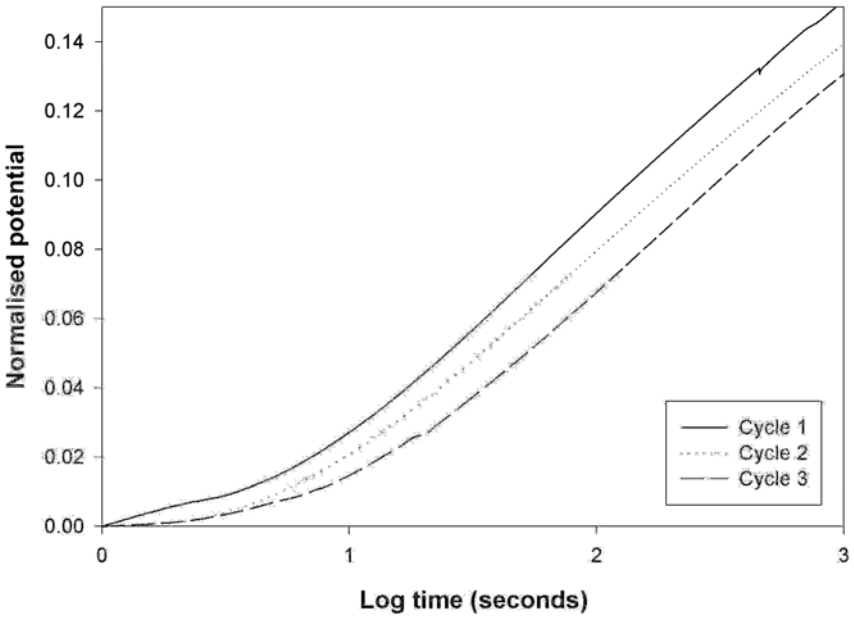

Figure 7

Rather than exhibiting a straight forward exponential decay of the active sites, the repassivation process appears to involve two phases; the first being more rapid with a larger decay constant which varies according to the surface damage inflicted, followed by a period of slower constant decay, indicated by all the plots having a constant slope. It is important to note that load increments were carried out at a constant strain rate. Hence, certainly in the plastic region, as load increments occur at progressively higher loads, the time to apply each 1 kN step increases. Hence, the competing mechanisms of film disruption and passivation will mean as the test proceeds to higher loads, the rate of production of fresh substrate material will reduce.

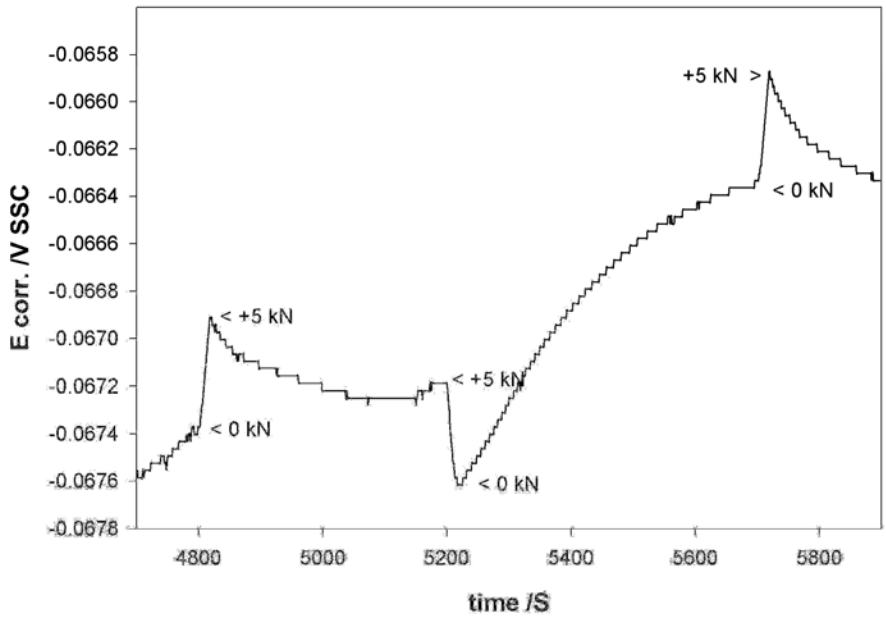

Figure 8

Another effect on the signal was observed during the loading and unloading cycles (Fig 8). This again was a millivolt range change but seemed to be present in most tests. An experiment was designed to check whether some of these electrochemical effects observed were actual manifestation of changes to the oxide film or whether these occurred as an artifact of the experimental procedure. A polished tensile test specimen was gold plated and the electrolytic cell positioned over the gold surface. This arrangement was allowed to settle over night and as expected from a noble metal surface, a very stable E_{Corr} was apparent from the data record. The load was then cycled between 0 and 5 kN and similar effects were noted on the signal as had been experienced with the polished stainless steel surface. The voltage perturbations were very much reduced and this was clearly due to the much lower currents involved with a gold-plated surface. Hence, those features on the E_{Corr} signal are understood to be an artifact of the cell/o-ring motion and consequent disturbance to the electrochemical double layer during the dynamic loading phase and not an indication of disturbances to the surface film. To complete this experiment, the gold film was lightly scratched, upon which, the open circuit potential fell rapidly indicating the increased activity of the newly revealed steel surface below.

Series Three Tests

Until now and for all test sequences, the specimens had been exposed to a relatively benign sulphate environment. This series involved changing the cell electrolyte to potassium chloride and using an SCC standard reference elctrode and thus exposing the austenitic stainless steel to the more challenging chloride ion. Preliminary tests involved the addition of 1 ppm Cl^- and a constant strain experiment, well into the plastic zone, did not indicate that this low level of chloride exacerbated the situation. A further specimen was polished and allowed to passivate in air for four days. The electrolyte was replaced with a 1M solution of KCl (35,500 ppm of Cl^-). This specimen was loaded to 5 kN and held at this constant level for some six days. During this period, a number of data records were acquired and these exhibited long periods of stability and the occasional single or multiple bursts of negative going activity on the E_{Corr} signal, which has been attributed to pit and crevice formation.

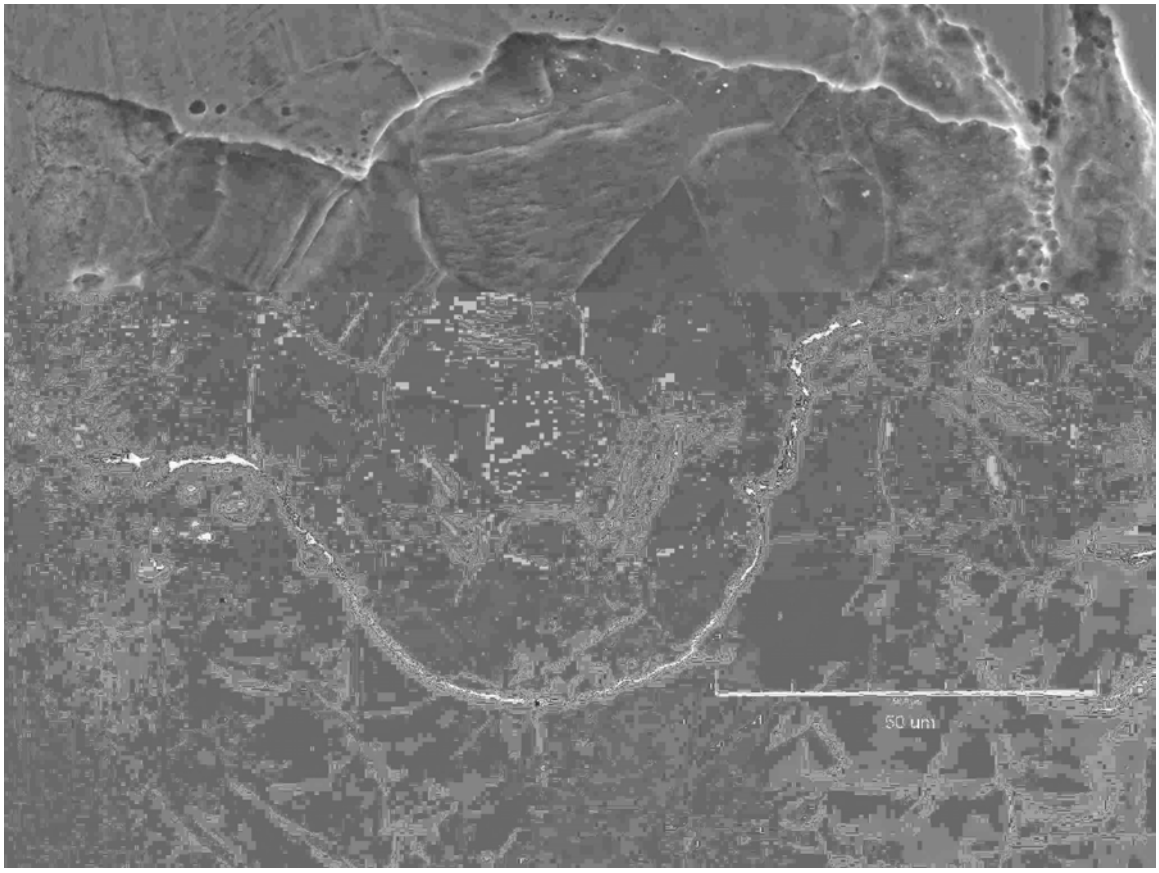

Plate 1

Observations on the Leitz microscope revealed one particular pit with a complex morphology. A section of this test specimen was removed and inserted in the SEM for more detailed observations. In the top left corner of the pit (Plate 1), an arrangement of clear slip steps can be observed. This sample was not dynamically loaded but taken to 5 kN and held at this load for a number of days in a reasonably concentrated Cl^- solution. Firstly, it is important to orientate these steps with respect to the applied constant load. If as they seem, these are truly slip steps, a question arises as to how these were formed under a static load condition.

Series Four Tests

The electrochemical instrumentation may be configured to pass a current through the specimen and hence, grow a film on the surface through an anodizing process. Given that previous experiments had pointed to not only, the surface finish but also the degree of passivation as being an important parameter, this technique would allow a more controlled and repeatable passive layer start point for experiments. As the currents involved are very low, it was important to isolate the specimen electrically from earth. Once this was achieved, a 1μA current was passed through the specimen for a set period. As passivation will continue after this period, the transfer time to the load frame and start of test needed to be minimized. An initial baseline test used a specimen with a freshly polished surface and hence no substantive passive film. This was followed by tests at anodizing times of 10, 20 and 30 minutes and by calculation, this yielded an expected oxide film thickness of 2, 4 and 6 nm, respectively. At the beginning of these anodizing processes, the potential measured was around –0.260 volts and as the film became thicker, this voltage increased and became more positive. To prevent disruption of the surface, it was important to keep this voltage below +0.8 volts, which is the pitting potential. For the 30 minute run, the final voltage was +0.788 volts. To anodize a thicker layer, it would be necessary to reduce the steady state imposed current to say 0.1 μA, which would give a commensurately lower voltage for a given film thickness. The results are similar to those reported in the Series One Tests, in that the thicker (30 minute) layer suffers a greater disruption (ΔE_{Corr}) than its thinner counterparts. It is interesting to note that when the initial degree of passivity is plotted against the degree of subsequent damage to the film through a constant strain rate test (Fig 9), the relationship is to a good approximation linear.

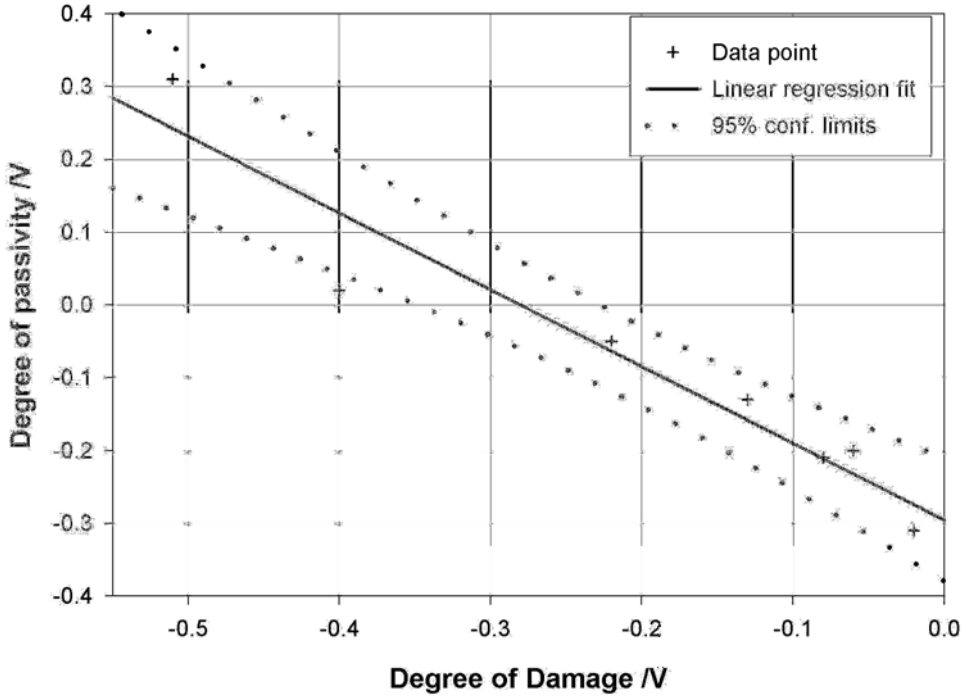

Figure 9

Conclusions

A full description is given of the new DASLER facility in the Nuclear Department has been given, together which its capabilities and flexibility of use. Four experimental series have been described that explore the nature of the passive oxide film which protects stainless steels. It has been demonstrated that failure of this film certainly occurs beyond the metal's yield point and repassivation competes with the generation of new substrate material in this dynamic process. Experiments have also shown that certain conditions will cause a breakdown of the film in the elastic region, through the mechanisms of crevice corrosion and pitting and it is the morphology of identified pits that are of particular interest.

Acknowledgements We are very grateful to Terry McCarthy, our Experimental Worker.

References

[1] K.R. Trethewey, M. Paton, Electrochemical impedance behaviour of type 304L stainless steel under tensile loading, Materials Letters 58 (2004) 3381-3384
[2] T. Hong, G.W. Walter, M. Nagumo, The observation of the early stages of pitting on passivated type 304 stainless steel in a 0.5 M sodium chloride solution at low potentials in the passive region by using the AC impedance method, Corrosion Science 39 (9) 1525
[3] T. Hong, M. Nagumo, The effect of chloride concentration on the early stages of pitting for type 304 stainless steel revealed by the AC impedance method, Corrosion Science 39 (2) 285
[4] R.M. Carranza, M.G. Alvarez, The effect of temperature on the passive film properties and pitting behaviour of a Fe-Cr-Ni alloy, Corrosion Science 38 (6) (1996) 909-925
[5] M. Cid, M. Puggali, H. Fatmaoui, M. Petit, A comparison of the depassivation of stainless steels by mechanical and electrochemical techniques, Corrosion Science 28 (1) 1988 61-68